BioNanoScience
https://doi.org/10.1007/s12668-019-0606-z

Green Synthesis, Characterization, and Investigation Antibacterial Activity of Silver Nanoparticles Using *Pistacia atlantica* Leaf Extract

Roonak Golabiazar[1] · Karwan Ismael Othman[2] · Karzan Mohammed Khalid[2] · Dlgash Hammad Maruf[1] · Sharmin Mustafa Aulla[1] · Pshtiwan Abdullah Yusif[3]

Abstract
The present article reports on a simple, economical, and green preparative strategy for synthesis silver nanoparticle with *Pistacia atlantica* leaf extract as a reductant, stabilizer, and capping agent. The green AgNPs were characterized by ultraviolet-visible (UV-Vis) spectrometer, energy dispersive X-ray diffraction (XRD), transmission electron microscopy (TEM), scanning electron microscopy (SEM) equipped with energy dispersive spectroscopy (EDX), and Fourier transform infrared (FTIR) spectrophotometer. The XRD pattern provided evidence for the formation of face-centered cubic structure with an average size of 17–18 nm. UV-Vis and FTIR were used to identify the biomolecules and capping reagents in the *Pistacia atlantica* leaf extract that may be responsible for the reduction of silver ions and the stability of the bioreduced nanoparticles. This work proved the capability of using biomaterial towards the synthesis of silver nanoparticle, by adopting the principles of green chemistry. In addition, the antibacterial activity of biologically synthesized nanoparticles was proved against gram-positive (*Streptococcus pyogenes* and *Staphylococcus aureus*) and gram-negative (*Salmonella paratyphi B*, *Klebsiella pneumonia*, *Escherichia coli*, and *Pseudomonas aeruginosa*) bacteria.

Keywords Green synthesis · Silver nanoparticles · Antibactrial activity · Gram-positive bacteria · Gram negative bacteria · Plant extract · *Pistacia atlantica* · Capping agent

1 Introduction

Nanotechnology is the fastest growing area of manufacturing in the world today and there is an increasingly frantic search for new nanomaterials and methods to make them. The research on synthesized nanomaterials and their characterization is an emerging field of nanotechnology, due to their huge applications in the fields of physics, chemistry, biology, and medicine [1–3]. The synthesized nanomaterials have been widely used in medicinal and technological aspects [4]. Silver nanoparticles among various metal nanoparticles have received significant consideration because they are effective antimicrobial agents that exhibit low toxicity and have diverse in vitro and in vivo applications [5, 6]. Silver nanoparticles (AgNPs) are increasingly used in various fields, including medical, food, health care, consumer, and industrial purposes, due to their unique physical and chemical properties [7]. These include optical, electrical, thermal, high electrical conductivity, and biological properties [8–11].

The earliest studies for the preparation of silver nanoparticles with a controlled size and shape are methods including the following: chemical reduction of silver ions generally in the presence of stabilizing agents [12] or without stabilizing [13], thermal decomposition in organic solvents [14, 15], reversed micelle processes [16, 17], photoreduction [18], ultrasonic radiation [19], and microwave irradiation [20, 21]. However, in most cases, the methods have potential hazards

✉ Roonak Golabiazar
rgolabiazar@yahoo.com

Karwan Ismael Othman
karwan.othman@soran.edu.iq

Karzan Mohammed Khalid
karzankardish@gmail.com

[1] Department of Chemistry, Faculty of Science, Soran University, Kurdistan Regional Government, Soran, Iraq

[2] Department of Biology, Faculty of Science, Soran University, Kurdistan Regional Government, Soran, Iraq

[3] Department of Chemistry, Faculty of Scienc, Salahaddin University, Kurdistan Regional Government, Salahaddin, Iraq

Published online: 07 February 2019

to health and environment. The green synthesis of nanoparticles has greatly reduced the use of physical and chemical methods. The development of green processes for the synthesis of nanoparticles is evolving into an important branch of nanotechnology [22, 23]. Green synthesis has multiple advantages over classical routes: it is cost effective, co-friendly, and does not require high pressure, energy, temperature, or the use of toxic chemical reagents [24, 25]. In recent years, green chemistry and biosynthetic methods have become more attractive ways to obtain AgNPs. These unconventional methods use either biological microorganisms, e.g., bacteria, fungi, marine algae, yeasts) or different alcoholic or aqueous plant extracts [26–29].

Plant-mediated synthesis of AgNPs is more advantageous compared to the methods that use microorganisms especially because they can be easily improved, are less biohazardous, and do not involve the elaborate stage of growing cell cultures [30–32]. Most importantly, the process can be suitably scaled up for large-scale synthesis of NPs [33].

Pistacia atlantica is found widely in the Zagrous Mountains, and particularly in western and northern Iran, eastern and northern Iraq, southern Turkey, and northern Syria in so-called Kurdistan [34]. *Pistacia atlantica* has antibacterial effects and is used in eczema treatments, for throat infections, kidney stones, asthma, and stomach ache and as an astringent, antipyretic, anti-inflammatory, antiviral, antimicrobial, pectoral, and stimulant [35, 36]. The earliest Phytochemistry studies and chromatographic fingerprints of this plant show that it may have fatty acids, flavonoids, phenolic compounds (such as gallic acid, quinic acid, tetragalloylquinic acid, trigalloylglucose acid) and triterpenoids, α-pinene, terpinolene, and starch which have been isolated from this species during the past decades [37, 38].

Here, we report a simple and eco-friendly antibacterial effects, procedure for the green synthesis of AgNPs, using *Pistacia atlantica* (originated from *Rawanduz* region of Kurdistan Regional Government, Iraq) leaf extract as a reductant, stabilizer, and capping agent. The choice of *Pistacia atlantica* leaves was made because of its benign nature and the presence of important functional groups allows AgNPs to be very stable and prevents the agglomeration of anchoring nanoparticles. The method used is simple, clean, free from toxic chemicals, and required only non-hazardous reactants like plant extract, water, and silver nitrate and is advantageous in large-scale production of silver nanoparticles. Silver nanoparticles were characterized by FE-SEM, EDX, TEM, XRD, and FTIR. Also, the optical absorption properties were measured by UV–visible spectrophotometer and an absorption peak observed in 445 nm due to surface plasmon resonance (SPR) of the silver nanoparticles. Finally, its antibacterial activity was investigated by the disk diffusion method for gram-positive (*Streptococcus pyogenes* and *Staphylococcus aureus*) and gram-negative (*Salmonella paratyphi B*, *Klebsiella pneumonia*, *Escherichia coli*, and *Pseudomonas aeruginosa*) bacteria.

2 Experimental

2.1 Materials

All chemical reagents used as starting materials were of analytical grade and purchased without any further purification. Silver nitrate ($AgNO_3$), hydrochloride acid (HCl), and ethanol (C_2H_5OH) were purchased from SD fine chemicals Pvt. Ltd., India company. The *Pistacia atlantica* leaves used in this study originated from Rawanduz region of Kurdistan Regional Government (KRG), Iraq. Distillated deionized water was used during this research. We have taken several bacterial species, gram-positive (*Streptococcus pyogenes* (ATCC19615) and *Staphylococcus aureus* (ATCC25923)) and gram-negative (*Salmonella paratyphi B* (ATCC8759), *Klebsiella pneumonia* (ATCC25922), *Escherichia coli* (ATCC25922), and *Pseudomonas aeruginosa* (ATCC27853)) from the Department of Biology, Soran University in KRG, Iraq.

2.2 Preparation of the Plant Extract

About 100 g of dried powder of *Pistacia atlantica* leaves transferred into a 1000-mL Erlenmeyer flask with 500 mL of distilled water along with boiling for 30 min. The aqueous extract was filtered and stored at 4 °C [34, 35, 37].

2.3 Green Synthesis of Silver Nanoparticles Using *Pistacia atlantica* Leaf Extract

In a typical synthesis of Ag NPs, 50 mL of *Pistacia atlantica* leaf extract was added dropwise to 50 mL of 0.003-mL/L aqueous solution of $AgNO_3$ with constant stirring at 80 °C and the color of the solution was changed from whitish to yellowish brown during the heating process due to excitation of surface plasmon resonance which indicates the formation of Ag nanoparticles [39, 40].

2.4 Screening of Antibacterial Activities

The well-diffusion technique [41] was used. Three hundred microliters of microbe cultures of age 18–24 h were added to Petri plates and nutrient agar was poured. Once the medium was solidified, holes were made and each hole was packed with different concentrations of nanoparticles ranging from 2.0 to 30.0 mg/mL. The plates were wrapped in parafilm tape and transferred to incubator and maintained at 37 °C for 24 h. The inhibition zones were then recorded in centimeters.

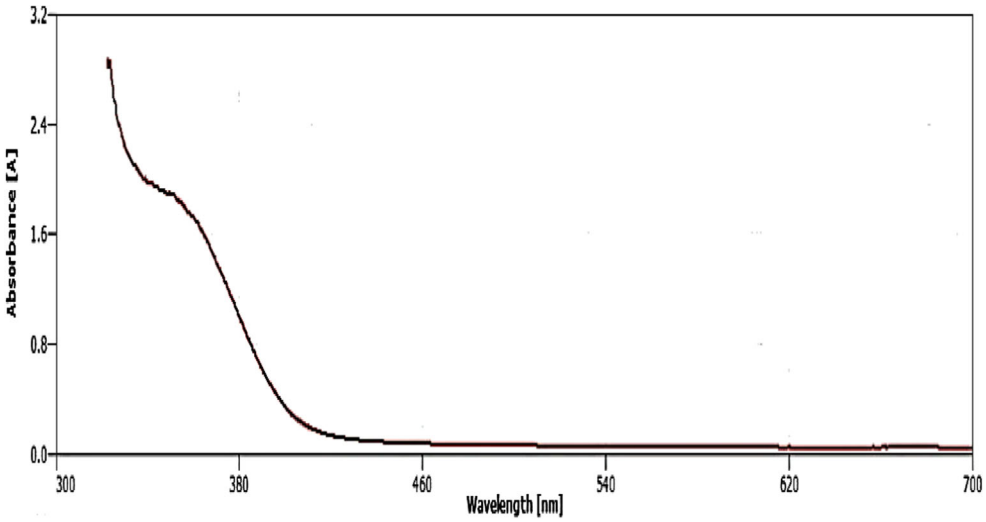

Fig. 1 UV–Vis spectrum of the aqueous extract leaves of the *Pistacia atlantica* at wavelength 300 to 700 nm

3 Measurement Techniques

The silver nanoparticles (AgNps) were characterized by FE-SEM, TEM, EDS, XRD, FTIR, and UV-Vis spectrometry.

3.1 Fast Emission Scanning Electron Microscopy with Energy Dispersive Spectroscopy

The morphology, particle dispersion, and chemical composition of the prepared nano-structures were investigated by fast emission scanning electron microscopy (FE-SEM) (Quanta 450) equipped with EDS at accelerating voltage 30 kV. Cross cut samples were prepared by fracturing the membranes in liquid nitrogen. A thin layer of gold was coated on all the samples before microscopic analysis.

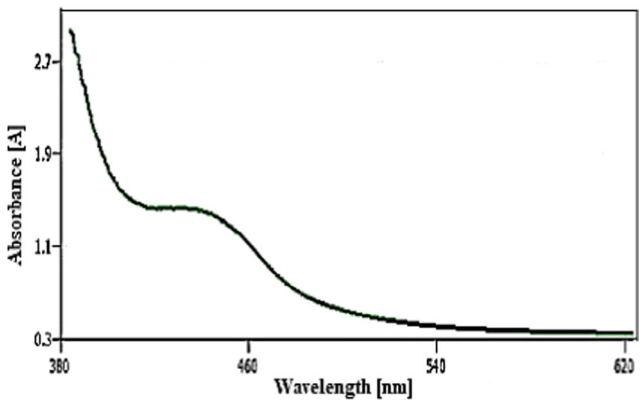

Fig. 2 UV–Vis spectrum of synthesized AgNPs using the *Pistacia atlantica* leaf extract at 300 to 640 nm

3.2 Transmission Electronic Microscopy

Bright field TEM images are recorded on a (Philips EM 120) transmission electron microscope at an accelerating voltage of 80 kV. The samples for TEM analysis are cut into slices of a nominal thickness of 100 nm using an ultra-microtome with a diamond knife at ambient temperature. The cut samples are supported on a copper mesh for this analysis.

3.3 X-Ray Diffraction

The X-ray diffraction (XRD) patterns of the sample were recorded at room temperature on a Philips powder diffractometer type (PW1373 goniometer) using Cu Kα ($\lambda = 1.54060$ Å) radiation with scanning rate of 2° min^{-1} in the 2θ range from 0° to 80°. Scanning was made for the selected diffraction peaks which were carried out in step mode (step size 0.01°, measurement time 0.5 s, accelerating voltage of 45 kV, and emission current of 40 mA measurement).

3.4 UV–Vis Spectroscopy

The periodic scans of the optical absorbance between 300 and 700 nm with a double-beam UV-Visible spectrophotometer (Carry 100 with tungsten halogen light sources) were performed to investigate the reduction of silver ions by leaf extract. The presented results were obtained at room temperature.

3.5 Fourier Transform Infrared Spectrophotometer

The binding properties of nanoparticles synthesized by co-precipitation method were investigated by Shimadzu FTIR spectroscopy (IRAffinity-1 Shimadzu Corp. A213750, Japan). Dried and powdered nanoparticles were pelleted with

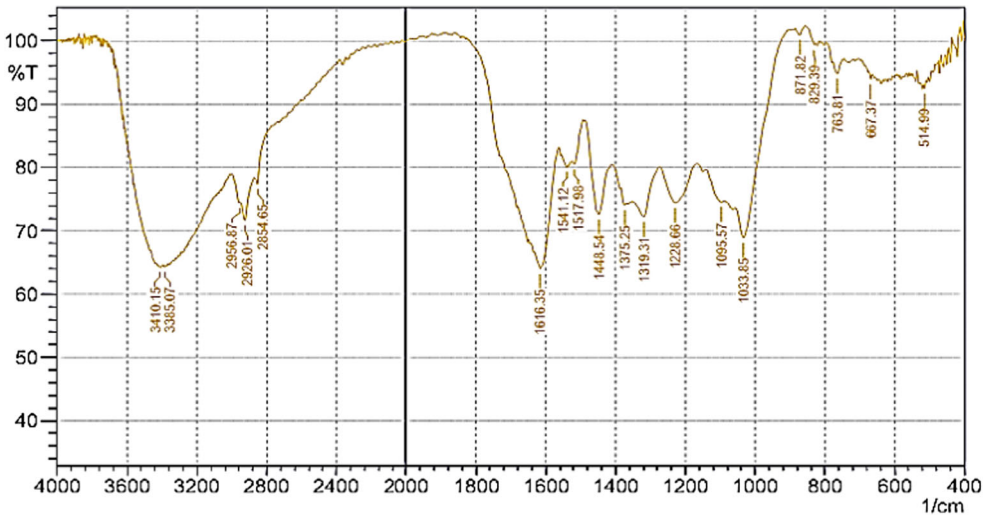

Fig. 3 FTIR spectra of the aqueous extract of leaves of the *Pistacia atlantica*

potassium bromide (KBr). The spectra were recorded in the wavenumber range of 400–4000 cm^{-1} and analyzed by subtracting the spectrum of pure KBr.

4 Results and Discussion

4.1 Characteristic of the Silver Nanoparticle

In this study, *Pistacia atlantica* leaf extract has been used as a reducing and stabilizing agent for the synthesis of silver nanoparticles. As can be seen in Fig. 1, the UV spectrum of leaf extract of the *Pistacia atlantica* shows absorption bonds at around 350 nm while AgNPs formed by leaf extract has a peak wavelength of 445–450 nm (Fig. 2). Reduction of silver ion to silver nanoparticles during exposure to the plant extracts could be followed by color change and spectroscopic techniques. Following the mixing of extract with aqueous solution of silver nitrate, it started to change the color from watery to dark brown due to the rapid change of the surface plasmon resonance phenomenon indicating the formation of silver nanoparticles. This change is denoted by the broadening of the peak which indicates the formation of polydispersed large nanoparticles due to slow reduction rates.

FTIR measurements were carried out to identify the possible biomolecules responsible for the capping and efficient stabilization of the silver nanoparticles synthesized by the plant extracts. The FT-IR spectra of *Pistacia atlantica* extract (Fig. 3) show several major peaks at 3385, 2926, 2854, 1616, 1375, 1095, and 1033 cm^{-1} and some other peaks approximately at around 510 to 1000 cm^{-1}. The broad and intense peak at 3385 cm^{-1} represents the –OH stretching vibration from phenolic compounds in the extract. The peaks observed at 2956, 2926, and 667 cm^{-1} are due to C–H stretching of

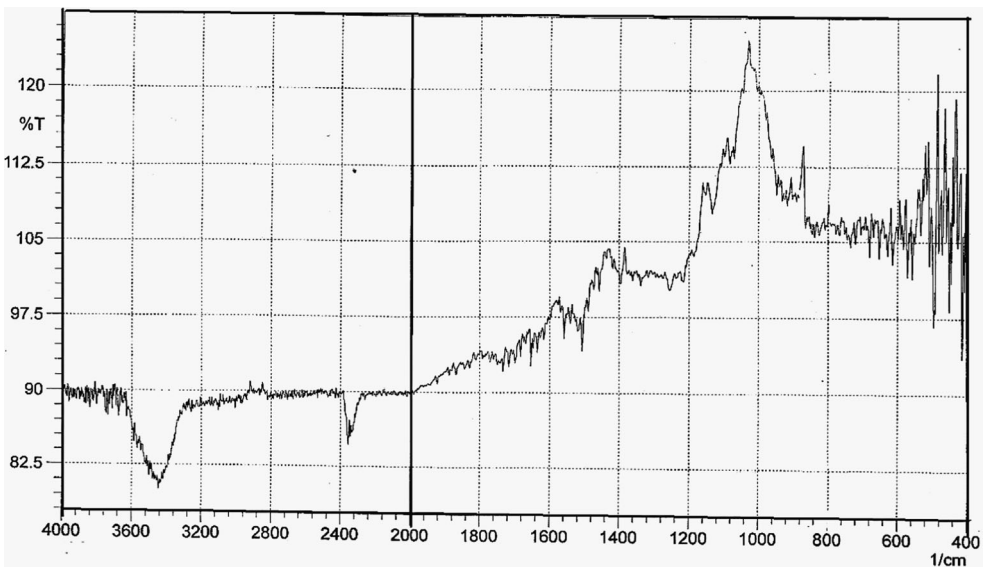

Fig. 4 FTIR spectra of synthesized AgNPs using the *Pistacia atlantica* leaf extract

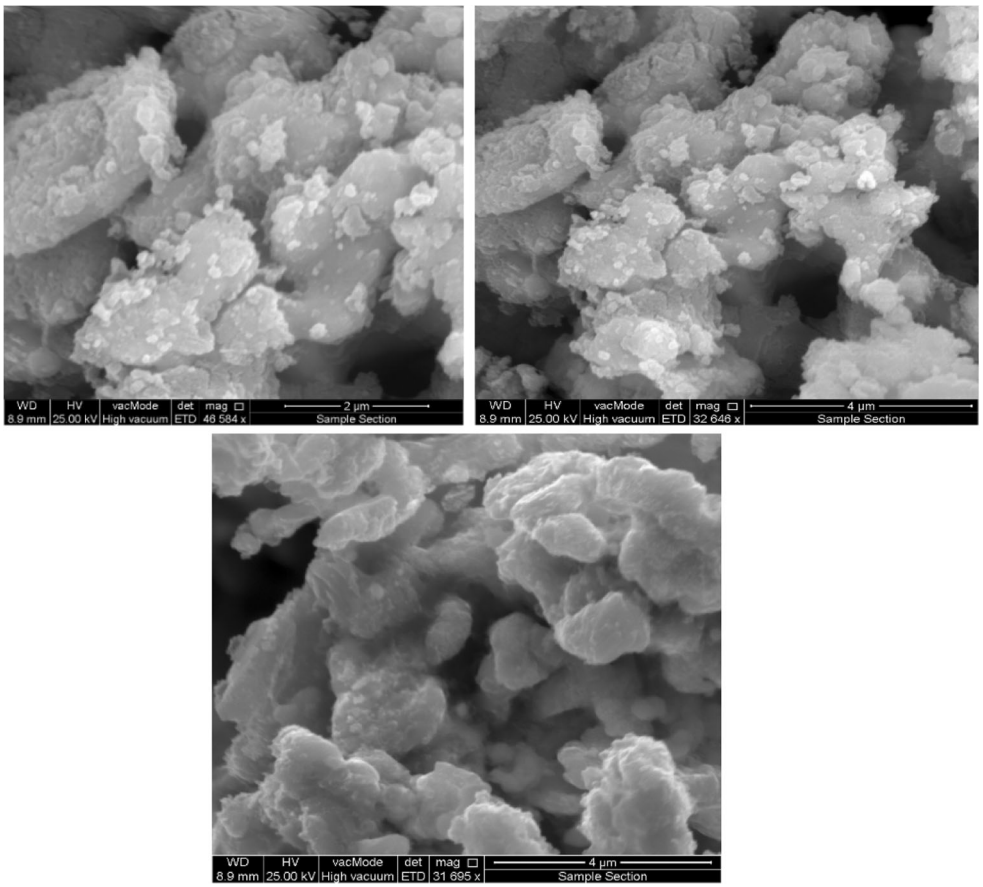

Fig. 5 SEM images of silver nanoparticles formed by *Pistacia atlantica* leaf extract

alkanes [42, 43]. The peak at 2854 cm^{-1} assigned to the N–H stretching vibration of amide II, while the three peaks at 1616, 1375, and 1033 cm^{-1} are probably attributable to the C=C aromatic stretch, C–O stretch, and C–O–C bending mode, respectively [44]. Furthermore, the FT-IR of AgNPs shows demonstrative differences in the shape and location of signals indicating the interaction between $AgNO_3$ and involved sites of biomolecules for production of nanoparticles (Fig. 4). After

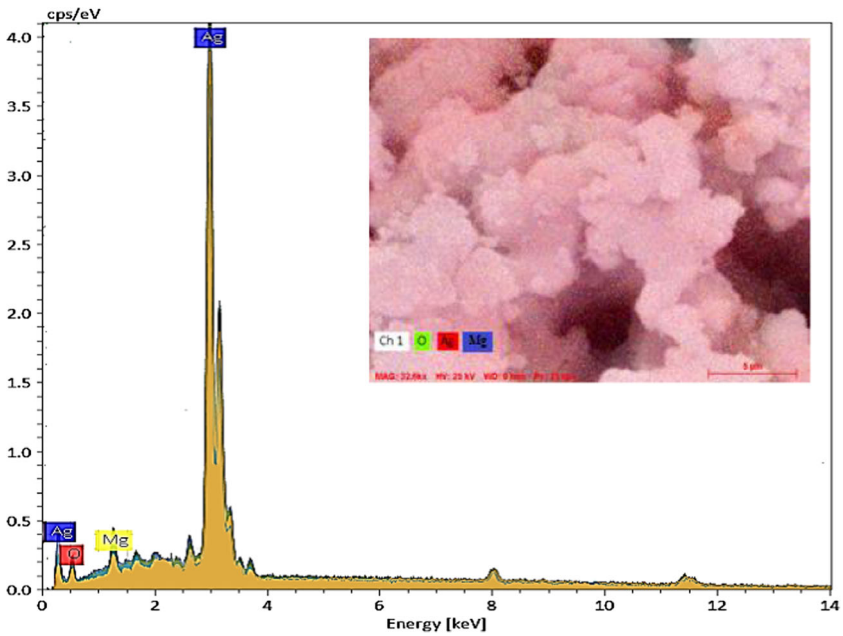

Fig. 6 Energy-dispersive X-ray spectroscopy EDS results of silver nanoparticles formed by *Pistacia atlantica*

Table 1 Elemental composition of AgNPs formed by *Pistacia atlantica* leaf extract from EDX

Spectrum	Weight of elements %		
	O	Mg	Ag
Ag 933	13.38604	3.463942	83.15002
Ag 934	10.87635	4.016734	85.10692
Ag 935	12.84705	3.162684	83.99026
Ag 936	9.763588	2.338785	87.89763
Mean	11.71826	3.245536	85.0362
Sigma	1.691669	0.700359	2.069174
Sigma Mean	0.845834	0.350179	1.034587

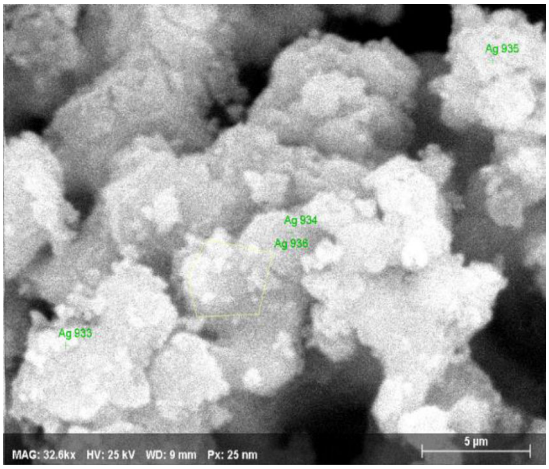

the Ag NPs formation, there are some shifts of valuable peaks such as the O–H, C–H, N–H vibration, and C–O stretch indicating that reduction occurred. Biomolecules could be adsorbed on the surface of metal nanoparticles, possibly by interaction through π-electrons interaction in the absence of other strong ligating agents.

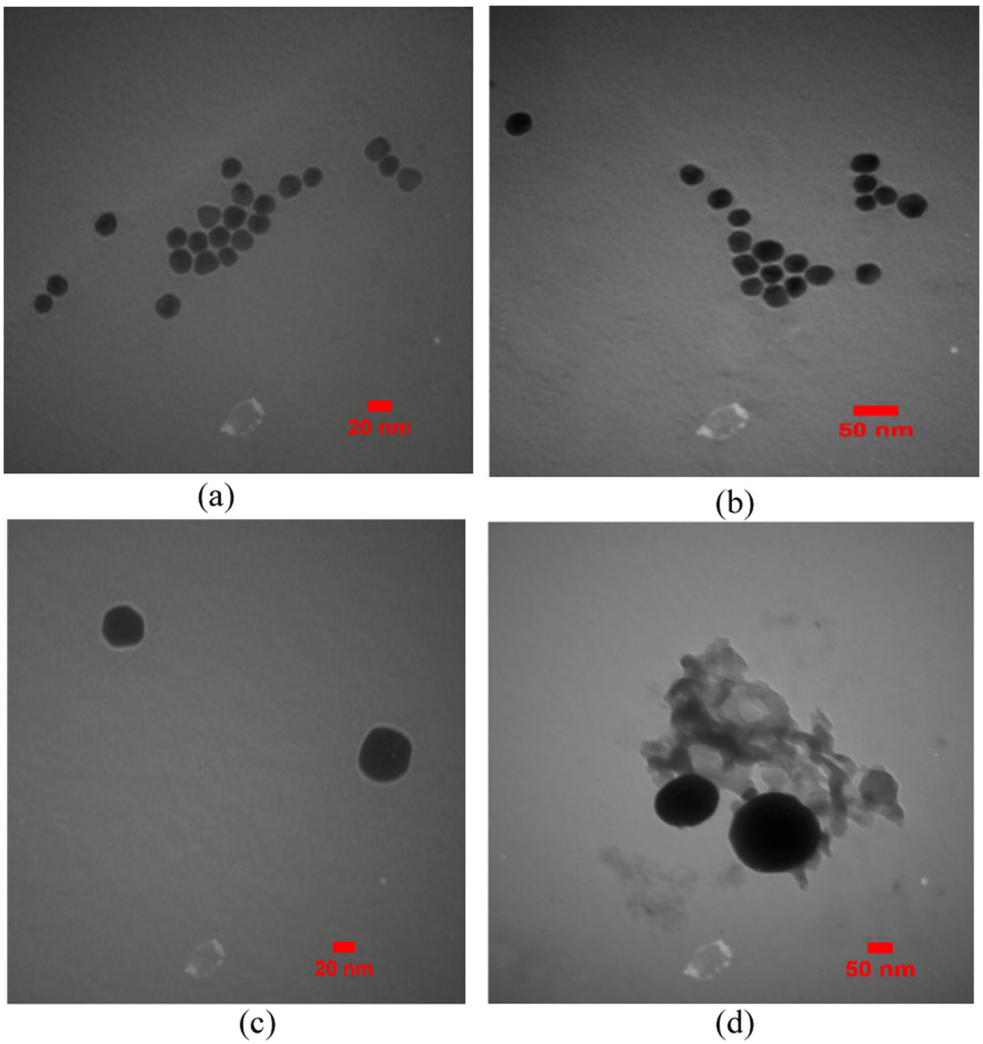

Fig. 7 **a**–**d** TEM image of silver nanoparticles at different resolutions 20 and 50 nm. **c**, **d** TEM images show organic layer surrounding silver nanoparticle as a capping agent. **d** TEM image shows clearly that the nanoparticle is having spherical shape

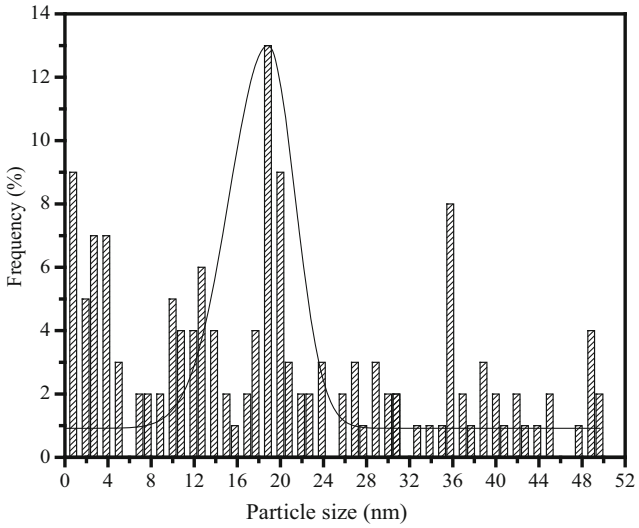

Fig. 8 Particle size distribution histogram of silver nanoparticles determined from TEM image

The SEM micro-graphs show the aggregate formation of AgNPs with spherical-like formation (Fig. 5). The surface composition of sample was qualitatively determined by energy dispersive X-ray spectroscopy (EDS) as shown in Fig. 6. The EDS analysis confirms that the aggregates are silver nanocrystals in that typical optical absorption peak is shown at approximately 3 keV. As can be seen in Fig. 6, the EDS spectra showed the strong peak of Ag and weaker signals for Mg and O were from biomolecules of *Pistacia atlantica*. This confirms the existence of only Ag content indicating no silver oxide formation in the sample. The composition components of AgNPs formed by co-precipitation synthesis are shown in Table 1.

The morphology of the biosynthesized AgNPs was displayed by TEM images in Fig. 7a–d. Most of the AgNPs are in spherical shape with a size less than 50 nm. Also from the images (Fig. 7c, d), thin layer of organic material from plant is observed as well as reported by some previous reports utilizing plant extracts [40, 45, 46]. As can be seen, Fig. 8 shows the histogram of particle size versus number of particles observed on TEM grid.

It is clear from the histogram that the mean particle size of AgNPs is 18.86 nm.

The silver molecules formed are necessarily subjected to XRD analysis for the measurement of size of these particles; Fig. 9 represents the XRD analysis of AgNPs nanoparticles. As can be seen in the Fig. 9, the peaks placed on diffraction angles at 37.94°, 44.12°, 64.28°, and 77.28° represent the synthesis of AgNPs with face-centered cubic structure that is, respectively, the reflex of crystalline planes (111), (200), (220), and (311) planes of face-centered cubic silver, which are closely matched with the reported reference value of JCPDS, file No. 98-018-0878. The strongest reflection comes from (111) plane, which denotes that the nanocrystals are (111) oriented as confirmed by SEM measurements in addition to the Bragg peak representative of face-centered cubic (FCC) silver nanocrystals. Hence, XRD pattern thus clearly illustrated that the silver nanoparticles formed in this present synthesis are crystalline in nature.

The crystallite size of the nanocrystalline samples was measured from the X-ray line broadening analyses using Debye-Scherrer formula after accounting for instrumental broadening (Eq. 1) [47, 48]:

$$D_{XRD} = \frac{0.9\lambda}{\beta\cos\theta} \tag{1}$$

where λ is the wavelength of X-ray used in Å, β is the line broadening at half the maximum intensity (FWHM in radians in the 2θ scale), θ is the Bragg angle, D_{XRD} is the crystallite size in nm. The average of the particle size of AgNps was found to be 17.01 nm using Scherrer equation from (111) plane. The lattice parameter "a" and interplanar spacing d_{hkl} are determined by Bragg's law (Eq. 2) and (Eq. 3) [49, 50]. The values obtained are shown in Table 2:

$$d_{hkl} = \frac{\lambda}{2\sin\theta} \tag{2}$$

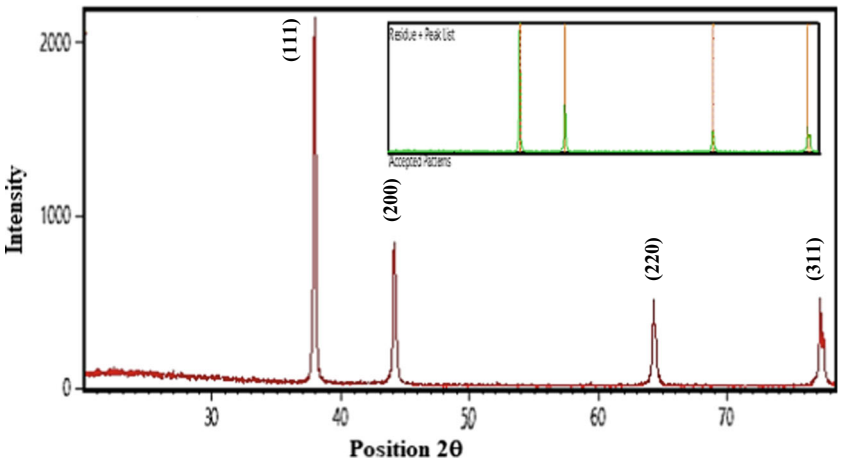

Fig. 9 XRD of silver nanoparticles formed by *Pistacia atlantica* and accepted pattern

Table 2 The values of observed 'd', crystalline size, dislocation density, strain, and *h*, *k*, *l* of AgNPs

Observed 2θ (°)	Observed *d* (A°) *a* = 5.417 A°	Crystalline size	Dislocation density (∂) ($\times 10^9$) lines/m^2	Strain (ε) ($\times 10^{-3}$) lines/m^4	*h*	*k*	*l*
37.94	2.36939	28.47	1.20	0.0204	1	1	1
44.12	2.05086	63.30	2.49	0.0416	2	0	0
64.28	1.44794	147.3	0.460	0.0036	2	2	0
77.26	1.23385	357.2	0.00783	0.0060	3	1	1

Table 3 Zone of inhibition for gram-positive and gram-negative bacterial strains in the presence of different AgNP concentrations at room temperature

Bacterial strains	Concentration of AgNPs (mg/mL)			
	2 mg/mL Zone of inhibition (cm)	13 mg/mL	22 mg/mL	30 mg/mL
Streptococcus pyogenes	0.6	0.6	1	1.5
Salmonella paratyphi B	0.7	0.8	0.8	1
Staphylococcus aureus	0.8	1.1	1	1.4
Klebsiella pneumonia	0.6	1.4	1.3	1.3
Escherichia coli	0.8	1	1.5	1.4
Pseudomonas aeruginosa	2.5	2.5	3	3.2

$$d_{hkl} = \frac{a}{\sqrt{h^2 + k^2 + l^2}} \tag{3}$$

Dislocation density (∂) is calculated with the crystalline size [50].

$$\partial = \frac{1}{D^2} \tag{4}$$

Micro strain arises due to the lattice misfit which varies on the deposition conditions and thus it is calculated by the formula [48, 49].

$$\varepsilon = \frac{(\beta \cos\theta)}{4} \tag{5}$$

We have observed that dislocation density has decreased with the increase in the crystallite size. Similarly, the micro strain has increased with the decrease in the crystallite size. These results are shown in the Table 2.

4.2 Bactericidal Activity of Silver Nanoparticle

The antibacterial activities of the AgNPs evaluated against several pathogenic bacteria (gram positive and gram negative) at concentration range (2.0 to 30.0 mg/mL in H_2O) of AgNPs are presented in Table 3 and Figs. 10 and 11. The result of antibacterial activity of AgNPs with different concentrations (2, 13, 22, and 30 mg/mL in H_2O) showed moderate antimicrobial activity against every of this pathogenic strains with zone of inhibition ranging from 0.6 to 3.2 cm (Table 3 and Fig. 11). The zone of the clearance around each well after the incubation period confirms the antimicrobial activity of the AgNPs extract.

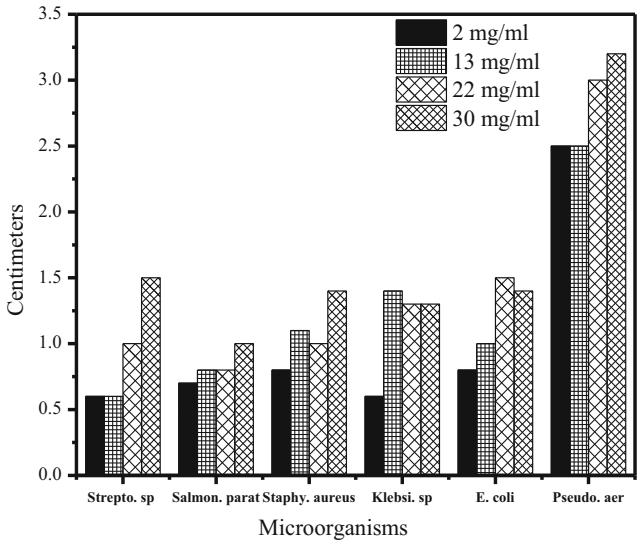

Fig. 10 Effect of antibacterial activities of the silver nanoparticle at different concentrations on zone of inhibition of microorganisms

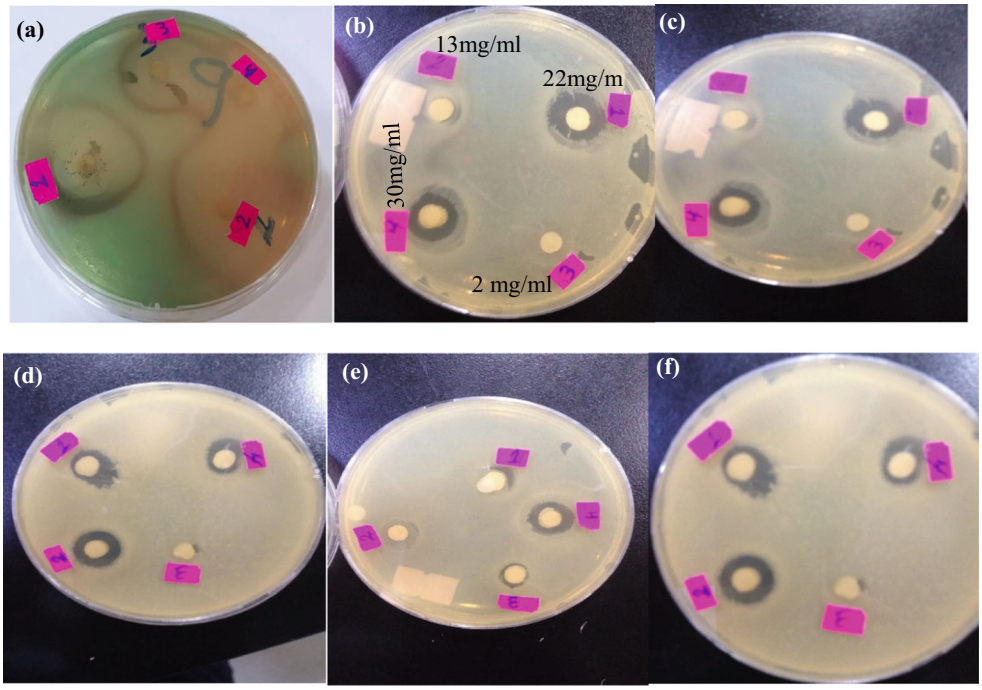

Fig. 11 Study of antibacterial activity (zone of inhibition) of silver nanoparticles formed by *Pistacia atlantica*. **a** *Pseudomonas aeruginosa*, **b** *Staphylococcus aureus*, **c** *Streptococcus pyogenes*, **d** *Escherichia coli*, **e** *Salmonella paratyphi B*, and **f** *Klebsiella pneumonia*

According to literature, antibacterial properties of the nanoparticles are attributed to the structural changes in the bacterial cell membrane and consequently facilitation of cell permeability by nanoparticles [51]. AgNPs might have been attached to the surface of the cell membrane of microorganisms, leading to the disturbance of its functions like permeability and respiration [52]. In this way, AgNPs with higher surface area and smaller size than the bacteria membrane pores cross them and have a significant effect on bacteria [52, 53]. In general, small nanoparticles have a larger surface area for interaction with bacteria, as compared to that of bigger particles, due to greater antibacterial activity.

5 Conclusion

Green silver nanoparticles were synthesized with a facile and rapid method by *Pistacia atlantica* leaf extract as a reducing and stabilizing agent. The green AgNPs were characterized by various techniques. The XRD result and TEM results confirmed that AgNP has the crystallite size about 17–18 nm. The dislocation density has decreased with the increase in the crystallite size. Similarly, the micro strain has increased with the decrease in the crystallite size. In this work, we present that the AgNPs have the potential to inhibit the growth of both gram-positive and gram-negative bacteria. In this way, AgNPs with higher surface area and smaller size than the bacteria membrane pores cross them and have a significant effect on bacteria.

Acknowledgments The authors would like to thank research center at Soran University for taken the SEM, FTIR, and UV-Vis spectra. Also Faculty of Biology for assistance with antimicrobial tests and for the constructive discussions.

Compliance with Ethical Standards

Conflict of Interest The authors declare that they have no conflict of interest.

Publisher's Note Springer Nature remains neutral with regard to jurisdictional claims in published maps and institutional affiliations.

References

1. Allafchian, A. R., Bahramian, H., Jalali, S. A. H., & Ahmadvand, H. (2015). Synthesis, characterization and antibacterial effect of new magnetically core–shell nanocomposites. *Journal of Magnetism and Magnetic Materials, 394*(2), 318–324.
2. Allafchian, A. R., & Jalali, S. A. H. (2015). Synthesis, characterization and antibacterial effect of poly (acrylonitrile/maleic acid)–silver nanocomposite. *Journal of the Taiwan Institute of Chemical Engineers, 57*(1), 154–159.
3. Song, J. Y., & S, K. B. (2008). Rapid biological synthesis of silver nanoparticles using plant leaf extracts. *Bioprocess and Biosystems Engineering, 32*(2), 79–84.
4. Aparna, G. S., Subbaiah, K. V., Saigopal, D. V. R., Subba Rao, Y., & Varada Reddy, A. (2014). Efficient and robust bio fabrication of silver nanoparticles by Cassia alata leaf extract and their antimicrobial activity. *Journal of Nanostructure in Chemistry, 82*(1), 1–9.
5. Krishnaraj, C., Jagan, E. G., Rajasekar, S., Selvakumar, P., & Kalaichelvan, P. T. (2010). Synthesis of silver nanoparticles using Acalyphaindica leaf extracts and its antibacterial activity against

water borne pathogens. *Colloids and Surfaces B: Biointerfaces, 76*(1), 50–56.
6. Allafchian, A. R., Mirahmadi-Zare, S. Z., Jalali, S. A. H., Hashemi, S. S., & Vahabi, M. R. (2016). Green synthesis of silver nanoparticles using phlomis leaf extract and investigation of their antibacterial activity. *Journal of Nanostructure in Chemistry, 6*(2), 129–135.
7. Shiraishi, Y., & Toshima, N. (2000). Oxidation of ethylene catalyzed by colloidal dispersions of poly (sodium acrylate)-protected silver nanoclusters. *Colloids and Surfaces A: Physicochemical and Engineering Aspects, 169*(1), 59–66.
8. Gurunathan, S., Park, J. H., Han, J. W., & Kim, J. H. (2015). Comparative assessment of the apoptotic potential of silver nanoparticles synthesized by Bacillus tequilensis and Calocybe indica in MDA-MB-231 human breast cancer cells: Targeting p53 for anticancer therapy. *International Journal of Nanomedicine, 29*(2), 4203–4222.
9. Li, W. R., Xie, X. B., Shi, Q. S., Zeng, H. Y., Ou-Yang, Y. S., & Chen, Y. B. (2010). Antibacterial activity and mechanism of silver nanoparticles on Escherichia coli. *Applied Microbiology and Biotechnology, 85*(4), 1115–1122.
10. Mukherjee, P., Ahmad, A., Mandal, D., Senapati, S., & Sainkar, S. R. (2001). Ungus-mediated synthesis of silver nanoparticles and their immobilization in the mycelial matrix: A novel biological approach to nanoparticle synthesis. *Nano Letters., 1*(10), 515–519.
11. Chang, L. T. (1995). Studies on the preparation and properties of conductive polymers. VIII. Use of heat treatment to prepare metallized films from silver chelate of PVA and PAN. *Journal of Applied Polymer Science, 55*(5), 371–374.
12. Khan, Z., Al-Thabaiti, S. A., Obaid, A. Y., & Al-Youbi, A. O. (2011). Preparation and characterization of silver nanoparticles by chemical reduction method. *Colloids and Surfaces B: Biointerfaces, 82*(2), 513–517.
13. Liz-Marzan, L. M., & Lado-Tourino, I. (1996). Reduction and stabilization of silver nanoparticles in ethanol by nonionic surfactants. *Langmuir, 12*(15), 3585–3589.
14. Navaladian, S., Viswanathan, B., Viswanath, R. P., & Varadarajan, T. K. (2007). Thermal decomposition as route for silver nanoparticles. *Nanoscale Research Letters, 2*(1), 44–48.
15. Esumi, K., Tano, T., Torigoe, K., & Meguro, K. (1990). Preparation and characterization of biometallic Pd-cu colloids by thermal decomposition of their acetate compounds in organic solvents. *Journal of Materials Chemistry A, 2*(5), 564–567.
16. Pileni, M. P. (2000). Fabrication and physical properties of self-organized silver nanocrystals. *Pure and Applied Chemistry, 72*(1), 53–65.
17. Sun, Y. P., Atorngitjawat, P., & Meziani, M. J. (2001). Preparation of silver nanoparticles via rapid expansion of water in carbon dioxide microemulsion into reductant solution. *Langmuir, 17*(19), 5707–5710.
18. Henglein, A. (1998). Colloidal silver nanoparticles: Photochemical preparation and interaction with O_2, CCl_4, and some metal ions. *Journal of Materials Chemistry, 10*(1), 444–446.
19. Fatimah, I. (2016). Green synthesis of silver nanoparticles using extrac of Parkia speciosa Hassk pods assisted by microwave irradiation. *Journal of Advanced Research, 7*(6), 961–969.
20. Kahrilas, G. A., Haggren, W., Read, R. L., Wally, L. M., & Fredrick, S. J. (2014). Investigation of antibacterial activity by silver nanoparticles prepared by microwave-assisted green syntheses with soluble starch, dextrose, and arabinose. *ACS Sustainable Chemistry & Engineering, 2*(4), 590–598.
21. Yin, H. B., Yamamoto, T., Wada, Y., & Yanagida, S. (2004). Large scale and size controlled synthesis of silver nanoparticles under microwave irradiation. *Materials Chemistry and Physics, 83*(1), 66–70.
22. Raveendran, P., Fu, J., & Wallen, S. L. (2006). A simple and "green" method for the synthesis of au, ag, and au-ag alloy nanoparticles. *Green Chemistry, 8*(1), 34–38.
23. Armendariz, V., Gardea-Torresdey, J. L., Jose Yacaman, M., Gonzalez, J., Herrera, I., & Parsons, J. G. (2002). Gold nanoparticle formation by oat and wheat biomasses. *Proceedings of Conference on Application of Waste Remediation Technologies to Agricultural Contamination of. Water Resources, 2*(1), 397–401.
24. Kharissova, O. V., Dias, H. V., Kharisov, B. I., Perez, B. O., & Perez, V. M. J. (2013). The greener synthesis of nanoparticles. *Trends in Biotechnology, 31*(4), 240–248.
25. Joseph, S., & Mathew, B. (2015). Microwave-assisted green synthesis of silver nanoparticles and the study on catalytic activity in the degradation of dyes. *Journal of Molecular Liquids, 204*(2), 184–191.
26. Klaus, T., Joerger, R., Olsson, E., & Granqvist, C. G. (1999). Silver-based crystalline nanoparticles, microbially fabricated. *Proceedings of the National Academy of Sciences of the United States, 96*(24), 13611–13614.
27. Konishi, Y., & Uruga, T. B. (2007). Bioreductive deposition of platinum nanoparticles on the bacterium Shewanella algae. *Journal of Biotechnology, 128*(3), 648–653.
28. Willner, I., Baron, R., & Willner, B. (2006). Growing metal nanoparticles by enzymes. *Advanced Materials, 18*(9), 1109–1120.
29. Siddiqui, M., Redhwi, H., Achilias, D., Kosmidou, E., Vakalopoulou, E., & Ioannidou, M. (2018). Green synthesis of silver nanoparticles and study of their antimicrobial properties. *Journal of Polymers and the Environment, 26*(2), 423–433.
30. Ahmad, N., Sharma, S., Singh, V. N., Shamsi, S. F., Fatma, A., & Mehta, B. R. (2011). Biosynthesis of silver nanoparticles from Desmodium triflorum: A novel approach towards weed utilization. *Biotechnology Research International, 4*, 1),1–1),8.
31. Velusamy, P., Das, J., & Pachaiappan, R. (2015). Greener approach for synthesis of antibacterial silver nanoparticles using aqueous solution of neem gum (*Azadirachta indica* L.). *Industrial Crops and Products, 66*(2), 103–109.
32. Fang, P., Yanyan, H., Zhiguang, Y., Hao, Q., & Jinsong, R. (2018). Nucleotide-based assemblies for green synthesis of silver nanoparticles with controlled localized surface plasmon resonances and their applications. *ACS Applied Materials & Interfaces, 10*(12), 9929–9937.
33. Shankar, S. S., Rai, A., Ahmad, A., & Sastry, M. (2004). Rapid synthesis of au, ag, and bimetallic au core-ag shell nanoparticles using neem (Azadirachta indica) leaf broth. *Journal of Colloid and Interface Science, 275*(2), 496–502.
34. Veisi, H., Faraji, A. R., Hemmati, S., & Gil, A. (2015). Green synthesis of palladium nanoparticles using Pistacia atlantica kurdica gum and their catalytic performance in Mizoroki–heck and Suzuki–Miyaura coupling reactions in aqueous solutions. *Applied Organometallic Chemistry, 29*(8), 517–523.
35. Bozorgi, M., Memariani, Z., Mobli, M., Salehi Surmaghi, M. H., Shams-Ardekani, M. R., & Rahimi, R. (2013). Five Pistacia species (P. Vera, P. Atlantica, P. Terebinthus, P. Khinjuk,and P. Lentiscus): A review of their traditional uses, phytochemistry, and pharmacology. *The Scientific World Journal, 2013*(5), 1–33.
36. Samavati, V., & Adeli, M. (2014). Isolation and characterization of hydrophobic compounds from carbohydrate matrix of Pistacia atlantica. *Carbohydrate Polymers, 101*(3), 890–896.
37. Ahmed, Z. B., Yousfi, M., Viaene, J., & Dejaegher, B. (2016). Antioxidant activities of Pistacia atlantica extracts modeled as a function of chromatographic fingerprints in order to identify antioxidant markers. *Microchemical Journal, 128*(6), 208–217.
38. Gourine, N., Yousfi, M., Bombarda, I., Nadjemi, B., Stocker, P., & Gaydou, E. M. (2010). Antioxidant activities and chemical composition of essential oil of Pistacia atlantica from Algeria. *Industrial Crops and Products, 31*(2), 203–208.

39. Viswadevarayalu, A., Venkata, R., Venu, G., Sumalatha, J., & Adinarayana, R. (2015). Facile green synthesis of silver nanoparticles using Limonia Acidissima leaf extract and its antibacterial activity. *BioNanoScience, 5*(2), 433–444.
40. Ahmed, S., Ahmad, M., Swami, B. L., & Ikram, S. (2016). A review on plants extract mediated synthesis of silver nanoparticles for antimicrobial applications: A green expertise. *Journal of Advanced Research, 7*(1), 17–28.
41. Ponarulselvam, S., Panneerselvam, C., Murugan, K., Aarthi, N., Kalimuthu, K., & Thangamani, S. (2012). Synthesis of silver nanoparticles using leaves of Catharanthus roseus Linn. G. Don and their antiplasmodial activities. *Asian Pacific Journal of Tropical Biomedicine, 2*(7), 574–580.
42. Castellanos Gil, E., Colarte, A. I., Ghzaoui, A. E., Durand, D., Delarbre, J. L., & Bataille, B. (2008). A sugar cane native dextran as an innovative functional excipient for the development of pharmaceutical tablets. *European Journal of Pharmaceutics and Biopharmaceutic, 68*(2), 319–329.
43. Banerjee, P., Satapathy, M., Mukhopahayay, A., & Das, P. (2014). Leaf extract mediated green synthesis of silver nanoparticles from widely available Indian plants: Synthesis, characterization, antimicrobial property and toxicity analysis. *Bioresources Bioprocessing, 1*(4), 1–10.
44. Lin, L., Wang, W., Huang, J., Li, Q., Sun, D., & Yang, X. (2010). Nature factory of silver nanowires: Plantmediated synthesis using broth of Cassia fistula leaf. *Chemical Engineering Journal, 162*(2), 852–858.
45. Zayed, M. F., Eisa, W. H., & Shabaka, A. A. (2012). Malva parviflora extract assisted green synthesis of silver nanoparticles. *Spectrochim Acta Part A: Mol. Biomol Spectrosc, 98*(7), 423–428.
46. Roy, S., & Das, T. K. P. (2015). Lant mediated green synthesis of silver nanoparticles – A review. *International Journal of Plant Biology & Research, 3*(3), 1044–1055.
47. Koseoglu, Y., Alan, F., Tan, M., Yilgin, R., & Ozturk, M. (2012). Low temperature hydrothermal synthesis and characterization of Mn doped cobalt ferrite nanoparticles. *Ceramics International, 38*(5), 3625–3634.
48. Partha, P. G., Hanif, A. C., & Vijayanand, S. M. (2013). Sonochemical synthesis and characterization of manganese ferrite nanoparticles. *Industrial and Engineering Chemistry Research, 52*(50), 17848–17855.
49. Cullity, B. D. (1978). *Elements of x-ray diffraction* (2nd ed.). *Philippines*: Addison-Wesley.
50. Prabhu, Y. T., Venkateswara Rao, K., Kumari, B. S., Kumar, V. S., & Pavani, T. (2015). Synthesis of Fe_3O_4 nanoparticles and its antibacterial application. *International Nano Letters, 5*(2), 85–92.
51. He, Y., Ingudam, S., Reed, S., Gehring, A., & Strobaugh, T. (2016). Study on the mechanism of antibacterial action of magnesium oxide nanoparticles against foodborne pathogens. *Journal of Nanobiotechnology, 14*(1), 54–60.
52. Yousefi, A., Seyyed Ebrahimi, S. A., Seyfoori, A., & Mahmoodzadeh Hossein, H. (2017). Maghemite nanorods and nanospheres: Synthesis and comparative physical and biological properties. *BioNanoScience, 8*(3), 95–104.
53. Lee, H. L., Molla, M. N., Cantor, C. R., & Collins, J. J. (2010). Bacterial charity work leads to population-wide resistance. *Nature, 467*(7611), 82–86.